(24) Schaefer, D. W.; Joanny, J. F.; Pincus, P. *Macromolecules* **1980**, *13*, 1280.
(25) Hervet, H.; Léger, L.; Rondelez, F. *Phys. Rev. Lett.* **1979**, *42*, 1681.
(26) Léger, L.; Hervet, H.; Rondelez, F. *Macromolecules* **1981**, *14*, 1732.
(27) Callaghan, P. T.; Pinder, D. N. *Macromolecules* **1980**, *13*, 1085.
(28) Callaghan, P. T.; Pinder, D. N. *Macromolecules* **1984**, *17*, 431.
(29) Fleischer, G.; Straube, E. *Polymer* **1985**, *26*, 241.
(30) Wang, F. W.; Lowry, R. E.; Wu, E. S. *Polymer* **1985**, *26*, 1654.
(31) Ewen, B. et al. *Polym. Commun.* **1984**, *25*, 133.
(32) Edwards, S. F. *Proc. R. Soc. London, A* **1982**, *385*, 267.

Semidilute Solutions of Star Branched Polystyrene: A Light and Neutron Scattering Study

Klaus Huber, Siegfried Bantle,† Walther Burchard,* and Lewis J. Fetters‡

Institute of Macromolecular Chemistry, University of Freiburg, D-7800 Freiburg, FRG.
Received October 31, 1985

ABSTRACT: Small-angle neutron scattering (SANS) and static and dynamic light scattering have been carried out with a 12-arm polystyrene star in toluene at 20 °C in a concentration range up to 16%, which corresponds to a value of $c/c^* \simeq 8$, with $c^* = 1/[\eta]$ being the coil overlap concentration. Behavior similar to flexible linear chains is observed, with some characteristic differences: (i) a more sudden transition from the dilute behavior to a transient network is found, with $M_{app} \to \infty$ and a slow motion of diffusion with $D_{slow} \to 0$; (ii) around the gel formation concentration the complementary SANS measurements in the high-q region display a liquidlike structure factor. The results in the semidilute regime were found to depend on the time of centrifugation, which was applied for optical clarification. This observation is in agreement with older findings by Dautzenberg and Koberstein et al. with linear polystyrene in good solvents and indicates a metastable state of the semidilute solution.

Introduction

Solutions of macromolecules at higher concentrations have been the subject of research for a long time. The solution properties were found to be significantly different from those in the dilute regime, but a satisfactory theory for this regime was lacking. In 1975 des Cloizeaux[1] and later de Gennes[2] introduced a new concept by which a semidilute solution is supposed to be separated rather sharply from the regime of dilute solution. This conception has been cast more precisely in the form of a "phase diagram" by Adam and Delsanti.[4] The point of crossover in this diagram is determined by the coil overlap concentration c^*, which is affected by the geometric size of the individual molecules. There are different alternatives for defining this geometric size. According to de Gennes, one can assume with certainty

$$c^* \sim M/\bar{R}^3 \tag{1}$$

Furthermore, by the Fox–Flory relationship[3] the intrinsic viscosity is related to $\bar{R}^3/M$ as

$$[\eta] \simeq \phi\bar{R}^3/M \tag{2}$$

Thus it may be useful to set

$$c^* = 1/[\eta] \tag{3}$$

a suggestion first made by Utracki and Simha.[21] In these equations $\bar{R}$ is the root of the mean square end-to-end distance of a coil in a good solvent and the symbol $\sim$ means here and in the rest of the text "proportional to".

For concentrations sufficiently larger than c^*, a transient network of entangled chains is assumed, and, consequently, all measurable quantities must become independent of the chain length of the individual molecules. This demand leads to a number of simple relationships that in the recent past have been the subject of extensive examination.

In the past, linear chains, in particular polystyrene (PS),[4-9,32] have been the most extensively studied subjects of static and dynamic light scattering (LS) measurements. The scope of research has been extended recently to other flexible and semiflexible linear chains[8-17] in good solvents. In some previous papers,[15-17] the necessity of static LS in combination with dynamic LS experiments has been demonstrated. Here we report results obtained with a 12-arm-star branched PS in a concentration range up to $c = 16\%$, which corresponds to $c \simeq 8c^*$. The purpose of this study is to investigate the influence of branching on semidilute solutions.

In the following, we first review briefly the main statements of the scaling theory for semidilute solutions. Scaling laws are strictly valid only in the limit of $c \gg c^*$ and do not make any predictions about the crossover region. Experiments, on the other hand, often have to be carried out near this region, and it appears, therefore, of interest to study this particular regime in order to get a deeper insight into real semidilute solutions.

Predicted Properties in Semidilute Solutions

Osmotic Pressure. The demand of the molecular weight independence of the properties at $c \gg c^*$ led des Cloizeaux to a relationship for the osmotic pressure that reads

$$\Pi/RT = (c/M)f(c\bar{R}^3/M) = (c/M)f(c/c^*) = (c/M)(c/c^*)^m \tag{4}$$

This relationship is based on the impenetrable sphere approximation for the second virial coefficient

$$A_2 \sim \bar{R}^3/M^2 \tag{5}$$

For linear chains in very good solvents des Cloizeaux[1] finds $m = {}^5/_4$, which follows from the condition $\Pi \sim M^0$ and from

† Institute Laue—Langevin, Grenoble, France. Present address: Sandoz AG, Basel, Switzerland.
‡ Present address: Corporate Research—Science Laboratories, Exxon Research and Engineering Co., Annandale, NJ 08801.

0024-9297/86/2219-1404$01.50/0

$$\bar{R} \sim M^{3/5} \tag{6}$$

The scattering intensity from solutions is given by the relationship

$$Kc/R_\theta = (1/RT)(\partial\Pi/\partial c)_T \tag{7}$$

which together with eq 4 results in the power law

$$Kc/R_\theta \sim (c/c^*)^{1.25} \tag{8}$$

if $c \gg c^*$.

Correlation Length. The model of a semidilute solution used by des Cloizeaux[1] and de Gennes[2] is based on a *homogeneous structure*. This is a reasonable assumption if c is much larger than c^*, where a transient network of entangled chains can be expected. Such a homogeneous network can be fully described by only one correlation length ξ, which essentially corresponds to the mesh size of the network. Clearly, this mesh size no longer depends on the molecular weight of the polymer chain but decreases with increasing concentration. On the other hand, if the concentration becomes smaller than c^*, the correlation length ξ merges into the root-mean-square end-to-end distance $\bar{R}$ of the linear chain in a good solvent. Application of these two requirements to a scaling statement leads together with eq 1 and 6 to

$$\xi(c) = \bar{R}(c/c^*)^{-3/4} \tag{9}$$

Cooperative Diffusion. In contrast to the dilute solution where only mutual diffusion is observed, one can expect two types of motion in the semidilute regime. The first is the respirative motion of the network, which commonly is described by a cooperative diffusion coefficient D_{coop}. The second corresponds to the motion of the individual molecules through the entangled network. Irreversible thermodynamics gives the following equation for the translational diffusion coefficient:[19,20]

$$D \sim \bar{s}\partial\Pi/\partial c \tag{10}$$

In dilute solution, $\bar{s} = s \simeq M/f$ is the sedimentation coefficient (neglecting the buoyance term), and f is related to the hydrodynamic radius of the individual molecule. For an entangled network in semidilute solution, $\bar{s}$ is an apparent sedimentation coefficient, for which de Gennes derived the following equation:

$$\bar{s} \simeq (g/6\pi\eta_0\xi) \tag{11}$$

relating $\bar{s}$ to the correlation length ξ. Here $g = c\xi^3 N_A/M_0$ is the average number of segments in a volume that is spanned by ξ (sometimes called a "blob"), N_A is Avogadro's number, η_0 is solvent viscosity, and M_0 is the molar mass of one segment. Using eq 11 together with eq 10 and 4 and $g \sim c^{-5/4}$, one arrives at de Gennes' result[2]

$$D_{coop} \simeq (kT/6\pi\eta_0\xi) \tag{12}$$

and with eq 9

$$D_{coop} \simeq (kT/6\pi\eta_0\bar{R})(c/c^*)^{3/4} \tag{13}$$

for which we now write

$$D_{coop} = D_0(c/c^*)^{3/4}$$

Here use was made of the Stokes–Einstein relationship for D_0, the diffusion coefficient at infinite dilution

$$D_0 = (kT/6\pi\eta_0 R_H) \tag{14}$$

and the proportionality between the geometric distance $\bar{R}$ and the hydrodynamically effective radius R_H was taken into account.

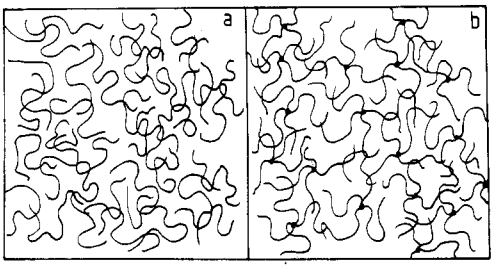

Figure 1. Semidilute solution for linear (a) and star branched molecules (b). Fixed cross-links are denoted with filled circles.

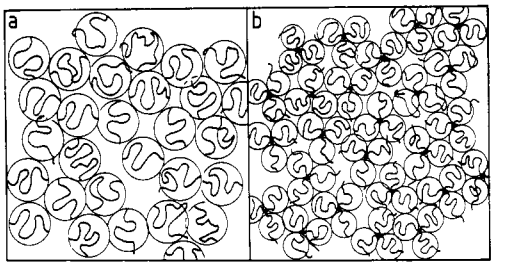

Figure 2. Overlap concentrations for linear (a) and for star branched molecules (b). The blobs are symbolized with circles.

Angular Dependence. The angular dependence of scattered waves is given by a Fourier transform of the density–density correlation function $g(r)$. Using the Ornstein–Zernike type radial correlation function given by Edwards[22]

$$g(r) \simeq (\xi/r)e^{-r/\xi} \tag{15}$$

one obtains

$$(R_\theta/Kc) = M_0 g/(1 + \xi^2 q^2) \tag{16}$$

with $q = (4\pi/\lambda)\sin(\theta/2)$, where λ is the wavelength in the medium and θ is the scattering angle. When Kc/R_θ is plotted against q^2, eq 16 predicts a straight line with

$$\text{slope} = \xi^2/M_0 g \tag{17a}$$

$$\text{intercept} = (1/M_0 g) = ((\partial\Pi/\partial c)/RT) \tag{17b}$$

Thus, the correlation length ξ and the "blob" molecular weight $M_0 g$ should be measurable from scattering experiments at appropriate wavelengths.

Special Properties of Star Branched Chains. All equations quoted so far were derived for flexible linear chains in a good solvent, and the question arises to what extent this picture can be transferred to star branched molecules. Figure 1 shows schematically a comparison of linear and star branched semidilute solutions. The main difference in the two structures is caused by the fixed cross-links of the star centers in addition to the points of entanglements, which are not fixed at a special point on the chain.

This fact has two immediate consequences. The first becomes apparent by comparing the two solutions at the overlap concentration c^*. While in the case of linear chain ξ becomes $\bar{R}$, the end-to-end distance, it is more reasonable to set for semidilute star molecules $\xi = \bar{R}_{arm}$, where $\bar{R}_{arm}$ is the root of the mean square distance of one arm end to the star center (see Figure 2). Second, if the arms are long enough, the power law (eq 6) for linear chains can be assumed for star molecules also. Therefore, a modification of eq 10a may be applicable to stars

$$\xi = \bar{R}_{arm}(c/c^*)^{-3/4} \tag{18}$$

If the star consists of shorter arms, chain stiffness and the influence of the star center cause competing effects on

Table I
Dilute Solution Properties of PS 4-12 in Toluene at 20 °C

$M_w \times 10^{-3}$	$A_2 \times 10^4$, mol cm^3 g^{-2}	$\langle S^2 \rangle$, nm^2	$D \times 10^7$, cm^2 s^{-1}	R_H, nm	$[\eta]$, cm^3 g^{-1}
467	2.09	320	2.39	15.2	49.7

the exponent in eq 6 and application of eq 18 then becomes rather questionable.

To our knowledge there is only one theoretical paper, by Daoud and Cotton,[18] treating the static properties of semidilute solutions of star branched molecules. They did not expect scaling to be valid. According to their concept, a semidilute solution of star branched polymers is not homogeneous but consists of at least two different regimes with different scaling behavior. The first regime consists of the undisturbed central parts of the star molecules, and, in the second regime, the arms of different molecules overlap and show behavior similar to semidilute linear molecules. In the limit of very long arms and high concentrations the second regime dominates the first regime, and the scaling laws for linear molecules may then be used to describe the entire solution.

Experimental Section

Samples. Light scattering experiments were carried out on a polystyrene (PS) 12-arm star sample of $M_w = 467\,000$ in toluene at 20 °C. The concentrations covered a region of $0.0008 < c < 0.16$ g/cm^3, where the latter is above $8c^*$. The intrinsic viscosity $[\eta]$ and all other dilute solution properties in toluene are collected in Table I. The overlap concentration is calculated from $[\eta]$ via eq 1, giving

$$c^* = 0.0201 \text{ g/cm}^3 \quad (19)$$

Neutron scattering experiments were carried out on the PS sample mentioned above, as well as on an additional PS 12-arm star molecule of $M_w = 149\,000$. Both samples were synthesized by one of us according to a procedure described in ref 24–26. They are identical with PS 4-12 and PS 6-12 of the previous paper.[23]

Light Scattering. The apparatus used for the simultaneous dynamic (DLS) and static light scattering (SLS) measurements is described elsewhere.[27] For $c < 0.005$ g/cm^3, a krypton ion laser Model 164 (Spectra Physics) with λ 647.1 nm[23] was used, and in the concentration range $c > 0.005$ g/cm^3, an argon ion laser with λ 488 nm Model 165 (Spectra Physics) was employed. The DLS data were recorded and evaluated by a special 4 × 4 bit autocorrelator/structurator from ALV Langen Co.[17,27]

The solvent, toluene, was distilled from sodium wire prior to use. After dissolution of the freeze-dried polymer, the solutions were kept at room temperature for at least 3 days. The polymer solutions were optically clarified by centrifugation of the scattering cells in a swinging bucket rotor, applying the floating technique.[28] Centrifugational conditions were 10 000 rpm for the durations indicated in Tables II and III. Experiments performed on 2 successive days gave reproducible results if no additional centrifugation was applied.

Neutron Scattering. Small-angle neutron scattering (SANS) measurements were performed at the Institute Laue–Langevin (ILL) in Grenoble, France. All experiments were done with the instrument D-17, which was equipped with a 64 × 64 cell matrix assembly[29] for detecting the scattering intensity. The sample–detector distance was 2.7 m and the neutron wavelength was 1.0 nm. Data treatment was carried out at the ILL as usual.[30] Cyclohexane-d_{12} and toluene-d_8 from Merck, Sharp, and Dohme (Canada) with 98% deuteration were used without further purification.

Evaluation of Light Scattering Data. The solutions exhibited a fluorescence when λ 488 nm was used for the primary beam. This fluorescence, which is also found with common linear PS, increased with the sample concentration and became significant if $c > 0.015$ g/cm^3. We applied a correction by determining the fluorescence intensity as function of the sample concentration. Normalization, using the respective standard scattering intensity from toluene, made it possible to collect the data in a calibration curve, which then was used for correcting Kc/R_θ values. In some cases, a few measurements were carried out with an interference filter fixed in front of the photomultiplier in order to check the validity of the calibration curve. The uncertainty of extrapolated $Kc/R_{\theta=0}$ in Figure 5 is estimated at ±5%.

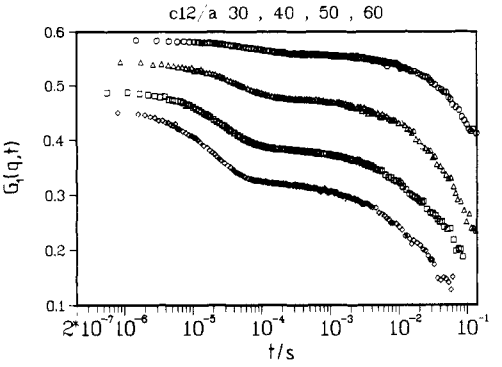

Figure 3. Typical set of time correlation functions $G_1 = (\langle i(0)i(t)\rangle - \langle i(t)\rangle^2)/\langle i(t)\rangle^2$ for sample c12/a at four different angles: (○) 30°; (△) 40°; (□) 50°; (◇) 60°.

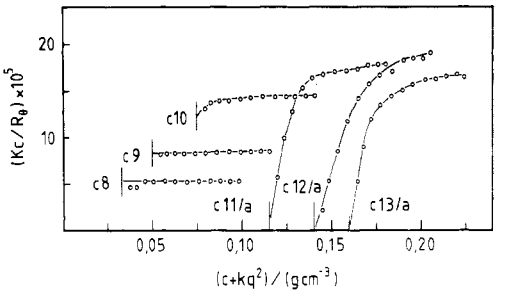

Figure 4. Zimm plot for the concentrations $c > c^*$ (not corrected for fluorescence). Time of centrifugation: 1 h at 10 000 rpm.

Data analysis of the intensity–time correlation function (TCF) $G_2 = \langle i(0)i(t)\rangle$, where $i(t)$ is the intensity as function of time, was performed in two different ways. First, a common on-line two-cumulant fitting was performed. Second, by applying the CONTIN program by Provencher[31] to the TCF, the relaxation spectrum was determined. If $c > 0.005$ g/cm^3, the TCF's were registered in the "multi-τ" mode,[17] by which delay times from a basic sample time τ to 512τ could be covered in one run. For $c > 5\%$, measurements at two different basic sample times became necessary and the two experimental curves had to be spliced together. Figure 3 exhibits four typical TCF's in this concentration range.

Results

Static Light Scattering. Figure 4 shows scattering curves measured without an interference filter and these are, therefore, only of qualitative relevance. They are presented to demonstrate the rather sudden onset of a strong angular dependence at low q values for c around 7.5%.

For higher concentrations the treatment of the scattering behavior presents some problems. The first is recognized from the shape of the scattering curves in Figures 4 and 5. These curves evidently consist of two sections that may be extrapolated separately. We introduce two different $Kc/R_{\theta=0}$ values, obtainable by different kinds of extrapolation. One is $1/M_{app}$ and corresponds to the apparent molecular weight that was obtained from the low-q-range extrapolation. The other, $1/M_{cor}$, was obtained from the flatter part in the high-q range. The angular dependence in the high-q range may be attributed to the structure factor of a "blob", which is defined in eq 16 through the correlation length; the extrapolated intercept is $1/M_{cor}$, which according to eq 17b would correspond to $(1/M_0 g)$,

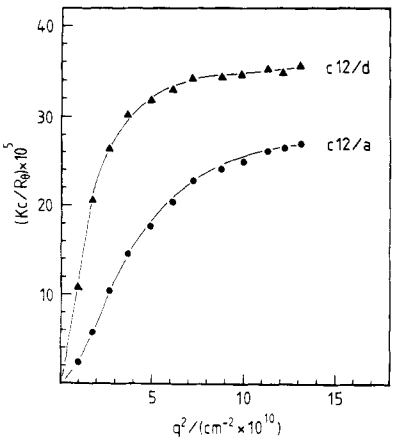

Figure 5. Influence of applied centrifugation time for optical clarification on the SLS profile of sample c12: (●) centrifuged for 1 h; (▲) centrifuged for an additional 15 h.

Table II
Diffusion Coefficient and Kc/R_θ at Zero Angle as a Function of Concentration[a]

sample	c, g cm^{-3}	$D_{cum} \times 10^7$,[b] cm^2 s^{-1}	$D_{con} \times 10^7$,[b] cm^2 s^{-1}	$Kc/R_{\theta=0} \times 10^5$, mol g^{-1}
c1	0.00081	2.47		0.248
c2	0.00163	2.56		0.281
c3	0.00244	2.65		0.325
c4	0.00407	2.80		0.416
c5	0.00530	3.05	3.25	0.587
c6	0.01326	3.90	4.14	1.418
c7	0.02010	4.63	5.37	2.424
c8	0.03315	6.07	6.72	5.807
c9	0.05026	7.55	8.32	9.676
c10	0.07479	7.52	10.43	16.5 19.7[c]

[a] Duration of applied centrifugal field is 1 h. [b] D_{cum} is obtained with a cumulant fit, whereas D_{con} is received from an application of the CONTIN program by Provencher.[31] [c] This value corresponds to $1/M_{cor}$ (for definition see text).

Table III
D_{coop} and $1/M_{cor}$ as a Function of Concentration at Different Durations of Applied Centrifugal Field

sample	c, g cm^{-3}	time of centrifug, h	$D_{coop} \times 10^7$, cm^2 s^{-1}	$1/M_{cor} \times 10^5$, mol g^{-1}
c11/a	0.1152	1	13.0	22.9
c11/b		1 + 3	12.9	29.5
c12/a	0.1406	1	13.4	17.1
c12/b		1 + 3	13.5	21.2
c12/c		1 + 3 + 3	13.7	28.9
c12/d		1 + 3 + 3 + 9	13.9	35.6
c13/a	0.1595	1	13.9	21.0
c13/b		1 + 3	14.0	34.0

where $M_0 g$ is the "blob molecular weight". This angular dependence very likely to some extent is superimposed on the tail of the initial part, which corresponds to much larger distances. Thus, the value for $1/M_{cor}$ may be too low and hence $M_{cor} > M_0 g$. Note that $1/M_{cor}$ is an *empirical* quantity that need not be identical with the "blob" molecular weight.

Figure 6 and Tables II and III contain these extrapolated values of $1/M_{cor}$ for measurements where the time of centrifugation, applied for optical clarification, was 1 h. Fairly accurate extrapolations over the whole q range could be made if $c < 0.0748$ g/cm^3; in this regime the angular dependence is very weak and lies within the experimental error. The extrapolation of the initial part of the scattering curve gave a finite value only in one case ($c = 0.0748$ g/cm^3). If $c > 0.0748$ g/cm^3 the extrapolation always yielded $1/M_{app} \cong 0$.

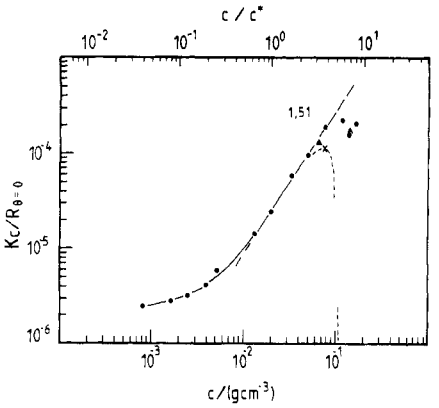

Figure 6. Concentration dependence of the static scattering behavior. If $c > 3c^*$, the values correspond to $1/M_{cor}$ except one point, denoted by (×), where extrapolation of the initial part in the scattering curve could be performed: (▲) measured with an interference filter for elimination of fluorescence. The straight line represents $Kc/R_{\theta=0} \sim (c/c^*)^{1.51}$ and the dashed curve the onset of bimodal behavior.

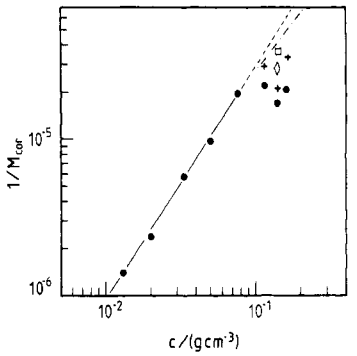

Figure 7. Influence of the duration of applied centrifugation periods on the concentration dependence of static scattering behavior: (●) 1 h; (+) 1 h + 3 h; (◇) 1 h + 2 × 3 h; (□) 1 h + 2 × 3 + 9 h. The straight line represents $Kc/R_{\theta=0} \sim (c/c^*)^{1.51}$ and the dashed–dotted line the des Cloizeaux law with an exponent of 1.25.

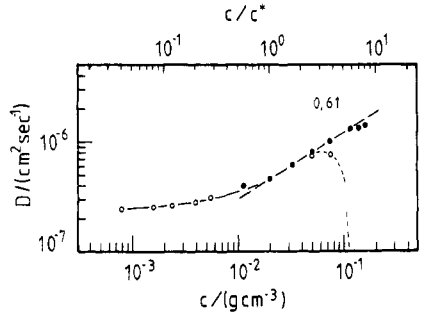

Figure 8. Concentration dependence of the dynamic scattering behavior: (●) CONTIN analysis, in the region with bimodal behavior only D_{coop} is shown; (○) results of a cumulant fit. The straight line represents $D_{coop} \sim (c/c^*)^{0.61}$.

An interpretation of the data for $c > 0.0748$ g/cm^3 is difficult, in particular because of an unusual behavior of these solutions when they are centrifuged for longer times. The influence of centrifugation time on the SLS and DLS is demonstrated in Figure 5 and Table III with the sample c12 as a typical example. Prolonged centrifugation raised the high-q section of Kc/R_θ and flattened the angular dependence. In Figure 7 the influence of centrifugation on the extrapolated $Kc/R_{\theta=0} = 1/M_{cor}$ values for the three highest concentrations is shown. In all cases the applied

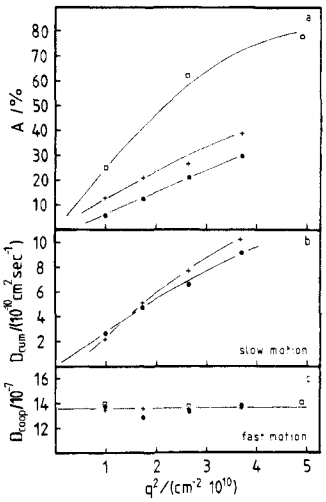

Figure 9. Influence of applied centrifugation time on the angular dependence of a CONTIN analysis with sample c12. (a) Shows the relative amplitude of the fast motion, (b) the slow motion, and (c) the fast motion. Symbols as in Figure 7.

gravimetric force caused an increase of $1/M_{cor}$; the points nevertheless remain below the curve with the slope of 1.51. For comparison, in the upper part a line is drawn with the des Cloizeaux slope of 1.25. Similar dependence on sample preparation was already observed by Dautzenberg et al.[33] and Koberstein et al.[34]

Dynamic Light Scattering. The DLS data is presented in Figures 8 and 9 and Tables II and III.

The diffusion coefficient was obtained from the first cumulant Γ at $q = 0$ according to the equation

$$D = \lim_{q \to 0} (\Gamma/q^2) \tag{20}$$

Up to a concentration of about 5% ($c \simeq 2.5c^*$) no angular dependence was observed, and with samples c9 and c10 the extrapolation toward $q \to 0$ could be carried out without problems. The diffusion coefficients so determined show the typical dilute solution behavior when $c < c^*$.

Figure 8 contains data points with two symbols, which indicate that the TCF's were analyzed by two different techniques. The open circles represent the results from the cumulant fit, while the filled circles give the results of the fast diffusive motion according to a more detailed analysis of the TCF with the CONTIN program of Provencher.[31] The two analysis techniques gave comparable results up to $c \simeq 5\%$. At this concentration, and even more pronounced for $c > 0.0748$ g/cm^3, a fast mode starts to deviate from the cumulant fit. Simultaneously, a slow mode appears. For c9 and c10 the rather low amplitude makes an accurate determination of the diffusion coefficient D_{slow} not feasible. For even higher concentrations, both a fast and a slow mode of motion always became detectable at finite angles. The fast-mode diffusion shows no angular dependence, but for the slow mode, a very pronounced q dependence was obtained. If $D_{slow}(q)$ is extrapolated toward $q \to 0$, one obtains $D_{slow}(q=0) = 0$, which would indicate no translational movement at all, as could be expected for an infinitely extended transient network. The fast motion may safely be interpreted as the predicted cooperative diffusion. The dashed line in Figure 8 indicates approximately the gel-setting concentration. Beyond this concentration evidently all conditions of a semidilute solution posed by des Cloizeaux and de Gennes are obeyed. The observed increase of D_{coop} with a power of (c/c^*) of 0.61, which is close to the exponents 0.67 and

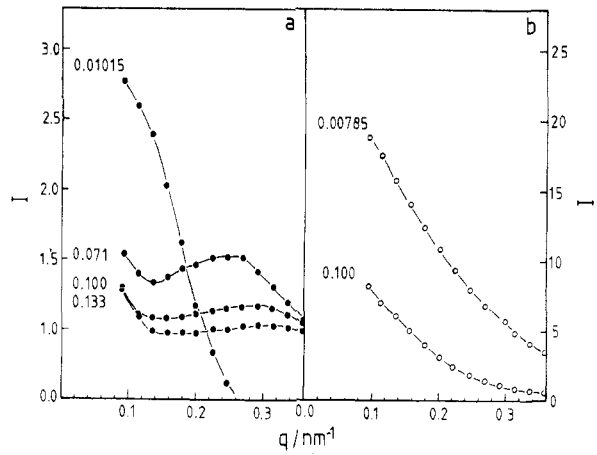

Figure 10. SANS intensity profiles of sample PS 4-12. (a) Contains the data received in toluene-d_8 at 20 °C. (b) Contains data obtained in cyclohexane-d_{12} at 34 °C. The numbers at the curves denote the concentrations in g/cm^3.

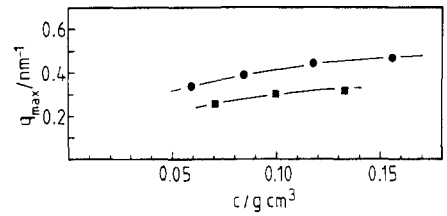

Figure 11. Concentration dependence of q_{max}, where maximum intensity occurs: (●) PS 6-12; (■) PS 4-12.

0.68 for linear PS in benzene,[4,32] is slightly smaller than predicted by des Cloizeaux.

Near the gel-setting concentration, the solution apparently is not yet in a full thermodynamic equilibrium, since the dynamic behavior, as well as the static, depends on the solution pretreatment. This is demonstrated in Figure 9 with the concentration of sample c12 of 0.1405 g/cm^3, which lies clearly in the mentioned gel region. The relative amplitude of the fast motion showed always the expected angular dependence and became in each case zero at $q = 0$; but it increases with the duration of centrifugation. The relaxation time of the fast motion remains constant within experimental error.

Small-Angle Neutron Scattering. SANS measurements were carried out with the sample PS 4-12 at 9 concentrations and with PS 6-12 at 10 concentrations. In both cases, the first six concentrations were chosen for the study of the dilute solution properties; the other data were obtained from concentrations near and well above c^*. The discussion here is confined mainly to the semidilute regime. The dilute solution behavior will be published in greater detail elsewhere.

Figure 10 represents the angular dependence for the sample PS 4-12 in toluene for the three highest concentrations and one concentration below c^*. These results are compared with corresponding measurements in cyclohexane at 34 °C. For $c > c^*$, these measurements display totally different angular dependences. While in cyclohexane a common behavior of scattering curves is obtained, a striking change above c^* is observed for the star molecules in the good solvent. This change is evidenced by the appearance of a maximum at intermediately large q values, denoted as q_{max}. This maximum is shifted to higher q as the concentration is increased. Figure 11 shows the variation for the two samples.

The occurrence of a maximum in a concentrated system is characteristic of a liquidlike structure. The position of

Table IV
Comparison of the Hydrodynamic Radius, R_H, the Radius of Gyration, $\langle S^2\rangle^{1/2}$, and the Equivalent Hard-Sphere Radius r_{HS} Calculated from the A_2 Values in Toluene with the Distance between Two Sphere Centers

c, g cm^{-3}	$L/2$,[a] nm	$\langle S^2\rangle_z^{1/2}$[a]	R_H[b]	r_{HS}[b]
	PS 4-12, M_w = 467 000			
0.071	14.7	12.7	15.2	16.2
0.100	12.9			
0.133	12.1			
	PS 6-12, M_w = 149 000			
0.060	11.4	7.3	8.25	9.3
0.085	10.5			
0.118	8.6			
0.156	8.2			

[a] From SANS measurements. [b] From LS measurements.

this maximum is determined in a complex manner by the *particle* and *interparticle* interferences, and it is difficult to relate the scattering pattern quantitatively to a mean interparticle distance.[35] Neglecting the particle scattering and assuming a face-centered cubic arrangement of particle centers, one can use the following equation[43] as a *rough* approximation of their mean distance:

$$L = (1.22\lambda/2 \sin(\theta_{max}/2)) = 1.22(2\pi/q_{max}) \quad (21)$$

Here q_{max} corresponds to the angle θ_{max} of the intensity maximum. These estimations for L are compared in Table IV with the equivalent hard-sphere diameter r_{HS} calculated from the second virial coefficients[23] via the equation

$$A_2 = (4\pi r_{HS}^3/3)4N_A/M^2 \quad (22)$$

and with the hydrodynamic radii[23] obtained from eq 14. The last column in Table IV contains the molecular radii of gyration received from SANS. These radii are somewhat smaller than obtained earlier by LS. This discrepancy may result from the rather high inaccuracy of $\langle S^2\rangle_z$ determination by LS for such small molecules but may also have some not yet understood origin.

Discussion

In this section we come back to the two main questions posed in the introduction, i.e., (i) how macromolecules behave in the crossover regime of the dilute to the semidilute concentration range, and (ii) the influence of the branched architecture on the properties of semidilute solutions.

The experimental data demonstrate that for $c > 3c^*$ a bimodal behavior is building up, both in the static and dynamic properties. This bimodal behavior is an indication of an inhomogeneous structure, at least in this crossover regime. This is opposed to the theoretical conception of a semidilute solution $c > c^*$, where the chains have formed an infinitely extended homogeneous network.

Indeed, the immediate formation of a network from individually dissolved macromolecules is very unlikely. Following the idea of the percolation theory, one comes to the conclusion that a cluster formation precedes the final gelation. There is, of course, a difference from the common percolation theory, since no real cross-links are formed; the points of entanglement are not locally fixed at a certain position of the chains, rather they are generated by topological constraints.

Concept of Clusters. The assumption of clusters recently proposed by several authors[9,15,16] allows a qualitative interpretation of the measurements.

(i) If clusters are present, two different characteristic lengths should be detectable, i.e., the correlation length ξ as defined in eq 9 and a length that characterizes the size of the cluster. The steep initial part of the angular dependence can be assigned to the cluster size, i.e., the radius of gyration of the cluster, and the flat section at larger q to the correlation length ξ. Moreover, the intercept gives then essentially the particle weight of the cluster and "blob", respectively. These clusters should increase in size with increasing concentration, and eventually a gel should be observed where the cluster molecular weight goes to infinity. For the star molecules M_w was shown to grow beyond all limits (i.e., $Kc/R_{\theta=0} \to 0$) if $c > 10\%$.

Only for the "blob" can the des Cloizeaux law be expected to hold, and this is indeed observed for linear PS in toluene.[1,41] For the star branched polymer, however, a larger exponent of 1.51 is obtained, while for other linear polymers, values lower than 1.25 were observed.[42]

(ii) The two scales of length must have also corresponding effects in dynamics. The occurrence of the slow motion in addition to the predicted fast one is very likely the consequence of the highly hindered motion of these clusters. In accordance with the static scattering behavior, the slow motion $D_{slow}(q)$ is strongly angular dependent and for $q = 0$ goes to zero at the onset of gelation (see Figure 9b). This is correlated with a decrease in the amplitude of the fast mode toward zero with decreasing q. The fast mode D_{coop} remains finite and angle independent, in agreement with eq 12, which related D_{coop} with the correlation length ξ and, thereby, also with M_0g. The angular dependence of $D_{slow}(q)$ is indicative for internal motions. This point is discussed in greater detail in a subsequent paper, which examines the time dependence of the TCF. Here we only wish to emphasize that for $c > 0.0748$ mg/cm^3 $D_{slow}(q=0)$ is zero, which means no translational motion at all.

The exponent of D_{coop} vs. c/c^* is predicted to be 0.75. This value has not been observed so far in any investigated polymer systems. The value of 0.68 for linear PS in toluene[32] and benzene[4] and 0.61 for the star branched PS are closest to this predicted value. In most other polymer/good solvent systems, lower exponents were observed. Only for the semiflexible cellulose–tricarbanilate chain was obtained an exponent of $\simeq 1$,[17] which lies close to the predicted value for a Θ-solvent system.[44] It should be emphasized, however, that this exponent can at this time only be determined in the concentration range $c < 4c^*$, which does not cover the typical semidilute regime, rather it corresponds to the crossover from dilute to semidilute behavior.

Nevertheless, the des Cloizeaux concept presents qualitatively the correct picture. For a better quantitative description, more specific calculations are required that take into consideration the fairly inhomogeneous structure of the solution in that crossover regime.

"Crossover". In this paper we have *defined* the overlap concentration by[21] $c^* = 1/[\eta]$. However, the onset of bimodal behavior does not occur until $3c^*$. It is striking that this concentration corresponds almost exactly to the overlap concentration that is obtained with the hydrodynamic radius R_H or the "equivalent" hard-sphere radius r_{HS} of the second virial coefficient, obtained by eq 22 (see Table IV). Both radii have nearly the same value in the limit of a very good solvent.[4,36,37] It may thus be advantageous to use this thermodynamically defined equivalent hard-sphere radius instead of $1/[\eta]$ in order to estimate an overlap concentration.

$$c_e = (M_w/N_A r_{HS}^3(4\pi/3)) \quad (23)$$

The quantity r_{HS} depends on the excluded volume β between individual pairs of segments. For a Θ-solvent one has $\beta = 0$ and $r_{HS} \to 0$, which indicates a free interpene-

tration of the coil. It appears conceivable that a much better quantitative description of solution behavior will become possible if a scaling with respect to c_e is employed rather than with c^*. See, for example, the light scattering data by Wiltzius et al.[46]

The findings by Koberstein et al.[34] for instance are also consistent with this concept. According to our suggestion, however, for Θ-solutions entanglement will not occur even if the coils strongly overlap. In other words, we think the cluster formation due to entangled chains does not have solely a topological reason but also depends on the strength of segment repulsion that may hinder disentanglement in a certain manner.

Structure Factor in Semidilute Solution. The picture of an "equivalent hard-sphere radius" may also be useful in interpreting the SANS data, which start to exhibit a liquidlike structure beyond a certain concentration. The interpretation of the q_{max} values, as given in Table IV, should be considered with caution since the actual data depend to some extent on the particular packing of the spheres and the unknown scattering function of the single chain in semidilute solution, as was demonstrated impressively by Guinier and Fournet.[35]

Fournet[38] quotes two characteristics concerning the intensity maximum in the scattering curves of a dense packing of hard spheres: (i) a shift of the exact maximum toward higher q values as the concentration increases, due to a decreased influence of the interparticle scattering function; (ii) a more pronounced form of the peak with increasing concentration.

Only the first of these two predictions was observed in our case. The fact that, contrary to the second prediction, just the opposite took place and that the shift of the maximum is also consistent with a decreased interparticle distance as the concentration increased led us to the following interpretation: behavior like hard spheres may occur only up to the overlap region and diminishes with increasing concentration because of the increase in coil overlap. In the melt state, hard-sphere behavior is no longer expected due to a full interpenetration of the chains. The experimentally observed liquidlike scattering behavior may not be explained by the concept of hard spheres in good solvent alone but is probably produced in combination with the impenetrability of the star centers. This conjecture is confirmed by the findings of Dautzenberg,[39] who did not observe an intensity maximum for linear PS in benzene at the corresponding concentrations; this indicates a solvent effect, which is too small to prevent a marked segment interpenetration.

Another example, in which a liquidlike structure factor was observed, is poly(vinyl carbanilate) in diethyl ketone.[40] Here special intramolecular interactions, e.g., H bonding, were assumed to be responsible for a highly hindered coil interpenetration.

Influence of the Sample Preparation. As the next point, the influence of the time of centrifugation on the state of the solution at $c > 3c^*$ is considered. It should be stated that no similar dependence exists in the dilute regime. Thus, the change in properties due to an external force on the system demonstrates a metastable structure of these solutions, and it is presently not possible to assign the true thermodynamic equilibrium. One gets the impression from Figure 7 that M_{cor} approaches a limiting value after very long times of centrifugation.

As already mentioned, M_{cor} is an empirical quantity that was obtained by extrapolation of an apparently asymptotic angular dependence. The q range accessible to light scattering is however, too small to warrant a determination of the real asymptote. Probably all curves found after different times of centrifugation will merge into one common line for very large q values, and this asymptote will correspond to M_0g. It seems that on centrifugation the gelled system rearranges from a rather dissolved structure into domains of more homogeneity in segment density.

The fast motion remains almost unaffected by the centrifugation procedure since the CONTIN analysis of the TCF's gives a much better separation of the fast mode of motion from the slow one than was possible for the two components in the SLS curves. This explains the difference in behavior of D_{coop} and $1/M_{cor}$ (see Table III). One may speculate that

$$M_{cor} \rightarrow (\text{const})c^{-1.25} \tag{24}$$

which corresponds to the equilibrium state. Only in this limit can the des Cloizeaux law be expected to hold. The dashed–dotted line in Figure 7 indicates the equilibrium semidilute behavior. The lower concentrations do not meet the condition $c \gg c^*$, as is required for the semidilute solution. The metastable nature of the more concentrated solutions poses the question: can *equilibrium* semidilute solutions be prepared without applying external forces on the system? The commonly prepared semidilute solutions are apparently more heterogeneous than the equilibrium solutions, as can be seen from the slopes in Figure 4.

Correlation to Physical Gelation. As a last remark, we wish to draw attention to a recent paper by Baer and his co-workers[45] on semidilute solutions of PS in several solvents. These authors reported in most cases, even for toluene, clear evidence for thermoreversible gelation. In contrast to these experiments our measurements have been performed well above their gel-setting temperature. Nevertheless, findings by Guenet et al.[47,48] indicate a correlation between the ability for thermoreversible gelation and the exhibition of enhanced low-angle scattering in semidilute solutions. These authors use the picture of a pregel state at higher temperatures, which is consistent with the conception of clusters used in the present paper.

Acknowledgment. A portion of this work was supported by a grant from the Polymers Program of the National Science Foundation (Grant No. DMR79-008299). W.B. and K.H. thank the Deutsche Forschungsgemeinschfat for financial support. We thank one of the referees for drawing our attention to the work by Baer et al.

Registry No. PS, 9003-53-6; neutron, 12586-31-1.

References and Notes

(1) des Cloizeaux, J. *J. Phys. (Les Ulis, Fr.)* **1975**, *36*, 281.
(2) de Gennes, P.-G. *Scaling Concepts in Polymer Physics*; Cornell University: Ithaca, NY, 1979.
(3) Fox, T. G.; Flory, P. J. *J. Chem. Phys.* **1949**, *53*, 197.
(4) Adam, M.; Delsanti, M. *Macromolecules* **1977**, *10*, 1229.
(5) Nose, T.; Chu, B. *Macromolecules* **1979**, *12*, 590.
(6) Yu, T. L.; Reihanian, H.; Jamieson, A. M. *Macromolecules* **1980**, *13*, 1590.
(7) Amis, E. J.; Han, C. C. *Polymer* **1982**, *13*, 1403.
(8) Brown, W.; Johnson, R. M.; Stilbs, P. *Polym. Bull. (Berlin)* **1983**, *9*, 305.
(9) Brown, W. *Macromolecules* **1984**, *17*, 66.
(10) Mathiez, P.; Weisbuch, G.; Mouttet, C. *Biopolymers* **1979**, *18*, 1465.
(11) Brown, W.; Stilbs, P.; Johnson, R. M. *J. Polym. Sci., J. Phys. Ed.* **1982**, *20*, 1771.
(12) Nose, T.; Tanaka, K. *IUPAC Int. Symp. Macromol. Chem., Prepr., 1982* **1982**, 715.
(13) Amis, E. J.; Janmey, P. A.; Ferry, J. D.; Yu, H. *Macromolecules* **1983**, *16*, 441.
(14) Selser, J. C. *J. Chem. Phys.* **1983**, *79*, 1044.
(15) Eisele, M.; Burchard, W. *Macromolecules* **1984**, *17*, 1636; *Pure Appl. Chem.* **1984**, *56*, 1379.

(16) Balloge, S.; Tirell, M. *Macromolecules* **1985**, *18*, 817.
(17) Wenzel, M.; Burchard, W.; Schätzel, K. *Polymer*, submitted.
(18) Daoud, M.; Cotton, J. P. *J. Phys. (Les Ulis, Fr.)* **1982**, *43*, 531.
(19) Yamakawa, H. *Modern Theory of Polymer Solution*; Harper & Row: New York, 1971.
(20) de Groot, S.; Mazur, P. *Thermodynamics of Irreversible Processes*; North Holland: Amsterdam, 1952.
(21) Utracki, L.; Simha, R. *J. Polym. Sci., Part A* **1963**, *1*, 1089.
(22) Edwards, S. F. *Proc. Phys. Soc.* **1966**, *88*, 265.
(23) Huber, K.; Burchard, W.; Fetters, L. J. *Macromolecules* **1984**, *17*, 541.
(24) Roovers, J. E. L.; Bywater, S. *Macromolecules* **1972**, *5*, 385.
(25) Hadjichristidis, N.; Guyot, A.; Fetters, L. J. *Macromolecules* **1978**, *11*, 668.
(26) Hadjichristidis, N.; Fetters, L. J. *Macromolecules* **1980**, *13*, 191.
(27) ALV-3000 Correlator/Structurator, supplied by ALV-Langen/Hessen, FRG.
(28) Dandliker, W. B.; Kraut, J. *J. Am. Chem. Soc.* **1956**, *78*, 2380.
(29) Institute Max von Laue–Paul Langevin, "Neutron Beam Facilities Available for Users", Jan 1981 ed.
(30) Ghosh, R. E. "A Computing Guide for SANS Experiments at the ILL"; 1981, GH 29T.
(31) Provencher, S. W. *Biophys. J.* **1976**, *16*, 27.
(32) Munch, J. P. et al. *J. Phys. (Les Ulis, Fr.)* **1977**, *38*, 971.
(33) Dautzenberg, H. *Faserforsch. Textiltech.* **1970**, *21*, 341.
(34) Koberstein, J. T.; Picot, C.; Benoit, H. *Polymer* **1985**, *26*, 673.
(35) Guinier, A.; Fournet, G. *Small Angle Scattering of X-Rays*; Wiley: New York, 1955.
(36) Han, C. C.; Akcasu, A. Z. *Polymer* **1981**, *22*, 1165.
(37) Huber, K.; Burchard, W.; Akcasu, A. Z. *Macromolecules* **1985**, *18*, 2743.
(38) Fournet, G. *Bull. Soc. Fr. Mineral. Cristallogr* **1951**, *74*, 39.
(39) Dautzenberg, H. *J. Polym. Sci., Polym. Symp.* **1977**, *No. 61*, 83; *Faserforsch. Textiltechn.* **1975**, *26*, 551.
(40) Burchard, W. *Polymer* **1969**, *10*, 29.
(41) Daoud, M.; Cotton, J. P.; Farnoux, B.; Jannink, G.; Sarma, G.; Benoit, H.; Cuplessix, R.; Picot, C.; de Gennes, P.-G. *Macromolecules* **1975**, *8*, 804.
(42) Burchard, W.; Wenzel, M.; Coviello, T.; Dentini, M.; Crescenzi, V. *Proceedings ESOPS 7 Conference*; Teubner Verlag: Leipzig, **1985**; Dresden, 1985.
(43) Reference 35, p 143.
(44) Brochard, F.; de Gennes, P.-G. *Macromolecules* **1977**, *10*, 1157.
(45) Tan, H.; Moet, A.; Hiltner, A.; Baer, H. *Macromolecules* **1983**, *16*, 28.
(46) Wiltzius, P.; Haller, H. R.; Cannell, D. S.; Schaefer, D. W. *Phys. Rev. Lett.* **1983**, *51*, 1183.
(47) Guenet, J.-M.; Willmott, N. F. F.; Ellsmore, P. *Polym. Commun.* **1983**, *24*, 230.
(48) Gan, J. Y. S.; François, J.; Guenet, J.-M. *Macromolecules* **1986**, *19*, 173.

Light Scattering from Polymer Blends in Solution. 2. Nondilute Solutions of Polystyrene and Poly(methyl methacrylate)

Takeshi Fukuda,* Minoru Nagata, and Hiroshi Inagaki

Institute for Chemical Research, Kyoto University, Uji, Kyoto 611, Japan.
Received October 3, 1985

ABSTRACT: Light scattering from polystyrene/poly(methyl methacrylate) blends in bromobenzene solution was studied over a wide range of molecular weight and concentration, extending to the spinodal of each blend while keeping the blend composition constant at about 50 vol %. All the solutions studied met the optical as well as thermodynamical symmetry conditions to such a high degree that the Flory–Huggins interaction parameter χ_{12} between the two polymers could be determined with very little experimental and theoretical ambiguities. The following facts have been disclosed: (1) For each pair of the polymers, there exists a characteristic concentration ϕ^* below which χ_{12} is approximately constant but above which it increases rather sharply. (2) ϕ^* is molecular weight dependent and has a strong correlation with the calculated "overlap" concentration that is supposed to characterize the crossover between the dilute and semidilute regimes. (3) In the dilute regime ($\phi < \phi^*$), χ_{12} exhibits a molecular weight dependence, which was quantitatively interpreted according to the two-parameter excluded volume theories, whereas in the semidilute or nondilute regime ($\phi > \phi^*$), χ_{12} is a function of concentration ϕ only. (4) The extrapolation of the log χ_{12} vs. log ϕ curve to $\phi = 1$ gives a value of about 0.030 as an estimate for χ_{12} in the bulk. This value is comparable to the dilute solution value obtained after being corrected for the excluded volume effects.

Introduction

Interactions between different polymers are, in many cases, difficult to characterize by using dry blends, especially when they are immiscible under usual conditions. Introduction of a suitable solvent brings about miscibility between otherwise immiscible polymers, thus rendering experimental approaches feasible. However, it also brings about complexities arising from polymer–solvent interactions.

In the early days, the role of the solvent in a ternary solution was considered merely to dilute polymers so as to reduce the number of polymer–polymer contacts, the solvent thermodynamic nature being unimportant. This optimistic view, which appeared to be consistent with early theoretical[1,2] and experimental[3,4] results, is no longer held in these days, for later studies[5–11] unequivocally showed that the phase-separation behavior of ternary solutions strongly depends on the solvent nature. For example, two polymers miscible in bulk can be made immiscible in solution when the solution affinities for the two polymers differ sufficiently.[9,10] Such strong solvent effects are liable to mask desired information on polymer–polymer interactions. In addition, possible dependences of the interaction parameters on solution compositions make rigorous analysis difficult in many cases.[6,7] For these reasons, our understanding of ternary solutions as yet remains very poor, and the rather pessimistic view seems to be prevailing that ternary solution data may not provide any quantitative or even qualitative information on polymer–polymer interactions.

In a previous paper,[12] we studied light scattering from polystyrene (PS)/poly(methyl methacrylate) (PMMA) blends in dilute solution of bromobenzene (BB). This solvent was chosen because it gives refractive index increments for the two polymers opposite in sign so that the interaction between the polymers can be selectively observed without interference by the polymer–solvent interactions. By this "optical Θ-state" method, we could

0024-9297/86/2219-1411$01.50/0